JGR Biogeosciences

RESEARCH ARTICLE
10.1029/2020JG005706

Marked Seasonal Changes in the Microbial Production, Community Composition, and Biogeochemistry of Glacial Snowpack Ecosystems in the Maritime Antarctic

A. J. Hodson[1,2], M. Sabacka[3], A. Dayal[1,4], A. Edwards[5], J. Cook[5], P. Convey[6], K. Redeker[7], and D. A. Pearce[6,8]

[1]Arctic Geology Department, University Centre in Svalbard, Longyearbyen, Norway, [2]Department of Environmental Sciences, Western Norway University of Applied Sciences, Sogndal, Norway, [3]Centre for Polar Ecology, University of South Bohemia, České Budějovice, Czech Republic, [4]Department of Geography, University of Sheffield, Sheffield, UK, [5]Institute of Biological, Environmental & Rural Sciences, Aberystwyth University, Aberystwyth, UK, [6]British Antarctic Survey, NERC, Cambridge, UK, [7]Department of Biology, University of York, York, UK, [8]Department of Applied Sciences, Northumbria University, Newcastle upon Tyne, UK

Abstract We describe seasonal changes in the biogeochemistry, microbial community and ecosystem production of two glacial snowpacks in the maritime Antarctic during a cold summer. Frequent snowfall and low, intermittent melt on the glaciers suppressed surface photosynthesis and promoted net heterotrophy. Concentrations of autotrophic cells (algae and cyanobacteria) were therefore low (average: 150–500 cells mL^{-1}), and short-term estimates of primary production were almost negligible in early summer (<0.1 μg C L^{-1} d^{-1}). However, order of magnitude increases in Chlorophyll *a* concentrations occurred later, especially within the mid-snowpack and ice layers below. Short-term primary production increased to ca. 1 μg C L^{-1} d^{-1} in mid-summer, and reached 53.1 μg C L^{-1} d^{-1} in a mid-snow layer close to an active penguin colony. However, there were significantly more bacteria than autotrophs in the snow (typically 10^3 cells mL^{-1}, but >10^4 cells mL^{-1} in basal ice near the penguin colony). The ratio of bacteria to autotrophs also increased throughout the summer, and short-term bacterial production rates (0.2–2000 μg C L^{-1} d^{-1}) usually exceeded primary production, especially in basal ice (10–1400 μg C L^{-1} d^{-1}). The basal ice represented the least diverse but most productive habitat, and a striking feature was its low pH (down to 3.3). Furthermore, all of the overlying snow cover became increasingly acidic as the summer season progressed, which is attributed to enhanced emissions from wet guano in the penguin colony. The study demonstrates that active microbial communities can be expected, even when snowmelt is intermittent in the Antarctic summer.

Plain Language Summary We consider the importance of snow as one of Antarctica's most important land-based ecosystems by describing snowpack ecosystem behavior at two sites upon a small maritime Antarctic ice cap. We show that a strong seasonal increase in the number of bacteria and snow algae occurs during the summer, despite the fact that our study coincided with a cold summer with frequent, wet snowfall events. These kept burying the snow algae, making photosynthesis difficult and allowing the bacterial community to dominate. An unexpected consequence was that the conditions also enhanced the decomposition of wet penguin guano, resulting in the release of organic acids whose subsequent deposition resulted in very acidic conditions within the snow matrix. Warmer summers with less snowfall will therefore experience completely different biological and chemical conditions in the snow habitat, emphasizing the climate sensitivity of this ice-hosted ecosystem.

Key Points:

- Regional nutrient enrichment by marine fauna influences the microbial ecology of glacial snowpacks in the maritime Antarctic during summer
- Cold summers with low melt and frequent snowfall reduce photosynthesis at the surface and allow bacterial production to dominate
- Persistent moisture supply to penguin guano enhances the effects of ammonium and organic acid deposition onto the snow ecosystem

Supporting Information:

Supporting Information may be found in the online version of this article.

Correspondence to:

A. J. Hodson,
Andrew.Hodson@unis.no

Citation:

Hodson, A. J., Sabacka, M., Dayal, A., Edwards, A., Cook, J., Convey, P., et al. (2021). Marked seasonal changes in the microbial production, community composition, and biogeochemistry of glacial snowpack ecosystems in the maritime Antarctic. *Journal of Geophysical Research: Biogeosciences*, *126*, e2020JG005706. https://doi.org/10.1029/2020JG005706

Received 19 FEB 2020
Accepted 14 JUN 2021

1. Introduction

1.1. Snow and Glacier Surface Ecosystems of the Antarctic

Snow and glacier ice represent the most expansive terrestrial habitat in Antarctica, yet biological and biogeochemical functioning upon their surface remain virtually unexplored. While the biology of snow upon the Antarctic ice sheet has received meaningful research attention (e.g., Carpenter et al., 2000; Michaud et al., 2014), its microbial ecology lags behind that of underlying cryoconite holes, supraglacial streams,s and lakes (e.g., Bagshaw et al., 2016; Hodson et al., 2013; Smith et al., 2017) or even englacial ice (e.g.,

D'Andrilli et al., 2017; Martinez-Alonso et al., 2019). These habitats have a fundamental dependence upon either snow accumulation prior to its transition into englacial ice, or snow ablation/deflation, prior to the onset of significant biological activity in summer (Hodson et al., 2015). Like any ecosystem, biological activity, nutrient assimilation and carbon transfers in Antarctica's near-surface icy habitats are greatly facilitated by the presence of meltwater. Melting glacial snowpacks thus represent a significant, but largely unaccounted component of the terrestrial ecology of Antarctica (Gray et al., 2020). Their study is given added importance by the fact that liquid water availability in the Western Antarctic Peninsula (WAP) has increased in response to the most rapid change in climate recorded within the Southern Hemisphere: nearly 3°C (0.56°C per decade) since the 1950s. A paucity of data from this region therefore means that we are poorly placed to consider the impact of the projected doubling of melt over the next three decades (Lee et al., 2017; Trusel et al., 2015; Vaughan, 2006), which will be dominated by the ablation of glacial snow and firn.

Most research on snowpack microbial ecology has been conducted in temperate regions or the Arctic (e.g., Ganey et al., 2017; Larose et al., 2013; Takeuchi, 2013; Thomas, 1972). Significant insights into glacial snowpack ecosystems have resulted, but there has been insufficient emphasis upon Antarctica. An increasing dominance of molecular studies of community structure or biogeography (e.g., Lutz et al., 2016; Malard et al., 2019) and biochemical or physiological processes (e.g., Davey et al., 2019; Lutz et al., 2015; Remias et al., 2016) is yielding important insights, but with limited integration with other important measurements of ecosystem functioning (such as primary and heterotrophic production) or biogeochemical and abiotic conditions. Furthermore, the so-called snow algae have received a disproportionate degree of attention (see Hoham & Remias, 2020), usually associated with the study of visually striking pigmentation which can darken the snow and thus enhance liquid water production for biological production (Cook et al., 2017; Dial et al., 2018). As a consequence, whole ecosystem studies are lacking and our understanding of controls upon spatial and temporal changes in the microbial community structure, biomass and functioning in Antarctic snow remains under-developed.

Glacial snowpacks in the Antarctic Peninsula region represent a habitat with strong seasonal variability in abiotic conditions, including the penetration of photosynthetically active radiation or harmful UV radiation, which change radically as snow grains undergo metamorphosis (Hodson, et al., 2017). Nutrient concentrations may also vary greatly, being very high in percolating meltwater at the start of summer, yet extremely dilute later on (Hodson, 2006; Nowak et al., 2018). Refreezing is also common, especially at higher elevations near the coast. Nutrient availability may be greatly enhanced by marine fauna, especially in the vicinity of penguin or seal colonies, as is the case in the present study (Greenfield, 1992; Hodson, 2006). Faunal emissions from the coastal periphery of Antarctica are known to have a regional effect as a consequence of longer-range aerosol deposition, especially with respect to nitrogen (Christie, 1987; Bokhorst et al., 2019; Legrand et al., 1998).

Whilst biological production at or near the snow surface can be important (Fogg, 1967; Thomas, 1972), even in global terms (Gray et al., 2020), two underlying habitats: slush and basal ice, deserve greater attention (Nowak et al., 2018). There is evidence to suggest that slush bacteria might be particularly productive, because percolation downwards from the upper snowpack brings nutrients and carbon toward the greater densities of cells often found in buried former melt surfaces (e.g., Amato et al., 2007). However, until measurements of net ecosystem production have been undertaken, the carbon balance of Antarctic snow and its underlying slush/ice habitats will remain unknown. We therefore present a study of seasonal changes in microbial community structure, biological production, and biogeochemical processes of snowpack ecosystems upon the Signy Island ice cap (South Orkney Islands, 60°S). In this study, we document seasonal changes in two glacial snowpacks representative of the broad range of melting and nutrient gradients found on the Antarctic Peninsula's west coast and associated archipelagos.

2. Materials and Methods

2.1. Study Site

Signy Island (60°S 45°W) is one of the four main islands in the South Orkney Archipelago. Approximately 32% of the 20 km^2 island area is currently ice-covered. The ice extent has reduced by 35%–45% since the 1950s on account of marked increases in mean annual air temperatures (Cannone et al., 2016; Noon

et al., 2003). The island has a wet, cold oceanic climate with annual precipitation of 350–770 mm, due to its position at the convergence of the cold Weddell Sea and the warmer Scotia Sea. Signy Island is very cloudy, due to orographic cloud formation over the nearby, mountainous Coronation Island, and thus receives on average only about 1.5 h of sunshine per day. The island's geology consists of metamorphosed sediments, mainly quartz-mica schist (Matthews & Maling et al., 1967). Due to the isolated oceanic and low altitude setting of Signy Island, its ice cap is more sensitive to fluctuations in climate change, especially since the mean annual air temperature, approximately—3°C, lies close to the melting point for ice. Of particular relevance to the present study is the presence of Adélie and Chinstrap penguin colonies on Gourlay Peninsula (Figure 1), where ca. 2000 breeding pairs are present (Dunn et al., 2016). The peninsula also becomes increasingly populated with fur seals as the summer progresses, with thousands of individuals arriving at the island by the end of summer (Waluda et al., 2010). Unsurprisingly, the permanent snow and glacier ice cover nearest the peninsula (hereafter Gourlay Snowfield) gradually turns dark red in response to these fauna fertilizing biological production by red snow algae, whose cell densities also become concentrated by snowmelt runoff. The same process occurs to a far lesser extent upon the other side of the island, but is still discernible (e.g., Tuva Snowfield: Figure 1). However, the South Orkney Islands experienced an unusually cold summer in 2012/2013 (Figure 2a), with temperatures fluctuating around the melting point upon the glaciers, causing far less snow ablation than is typical, and leaving the entire island surrounded by the largest extent of Antarctic sea-ice in recent history. High densities of snow algal cells therefore remained buried by snow for much of the summer and were barely discernible upon the surface.

2.2. Sampling

Two sampling sites (Gourlay Snowfield, 0.65 km^2 and Tuva Snowfield, 0.66 km^2) were established in early December 2012 on the Signy Island Ice cap. Samples of snow and ice were collected at sites shown in Figure 1. Snow sampling was complicated by multiple (typically 10 or more), discontinuous ice lenses up to 1 cm thick, and a basal ice layer composed of refrozen snowmelt up to 30 cm thick. Thus at each of the 18 snow pits visited (nine at each snowfield), the following samples were extracted: fresh surface snow (0–20 cm depth), bulk snow (lying from 20 cm depth to the base of the snow) and ice superimposed upon the previous summer surface at the base of the snowpack. These samples are hereafter referred to as "TOP, MID, and ICE" respectively. Samples were first collected in mid-December in order to characterize the entire winter's net accumulation upon the glacier surface. They were extracted using an autoclaved stainless steel knife that was also used to clean the snow pit face. The snow water equivalent content of each of these layers was determined using standard gravimetric methods described below. Repeat sampling surveys were conducted in mid-January and mid-February. Samples were returned to the laboratory at Signy in precleaned HDPE wide neck flasks and allowed to thaw at room temperature before immediate processing.

2.3. Snow and Ice Properties

Snow thickness was measured during the surveys (and opportunistically following fresh snowfall events) at all 18 snow pits using an avalanche probe (average of 3 readings per sampling site). Snow density was also assessed gravimetrically at each site using a 1 L pvc snow tube. The thickness of the superimposed ice was measured at the beginning and at the end of the season after excavation using an ice axe. In order to calculate the proportion of the total winter accumulation that was transformed into superimposed ice by surface melting followed by refreezing, its density was assumed to be 0.9 kg L^{-1}. The albedo of the snow in the spectral range 400–1,100 nm was approximated using an Apogee DQ100 pyranometer on a horizontal crossbar, alternately rotated through 180° to view upwelling and downwelling light. The ratio of upwelling and down-welling light was taken as an approximation of the surface albedo.

Key chemical properties of the snow were also determined during each survey, including pH, dissolved organic carbon (DOC), total dissolved inorganic carbon (TDIC) and ammonium (NH_4^+). The pH was determined using a Hanna Instruments (HI9025) meter and electrodes were calibrated weekly using fresh pH 4.01 and 7.01 buffer sachets (Hanna Instruments). The electrode was stored in pH 7.01 buffer between measurements and then allowed to stand in deionized water for 20 min prior to analysis. Thereafter, the electrode was rinsed in sample prior to immersion, stirring for 30 s and waiting for a stable reading. The other parameters required analysis of a filtered sample, which was undertaken immediately after melting.

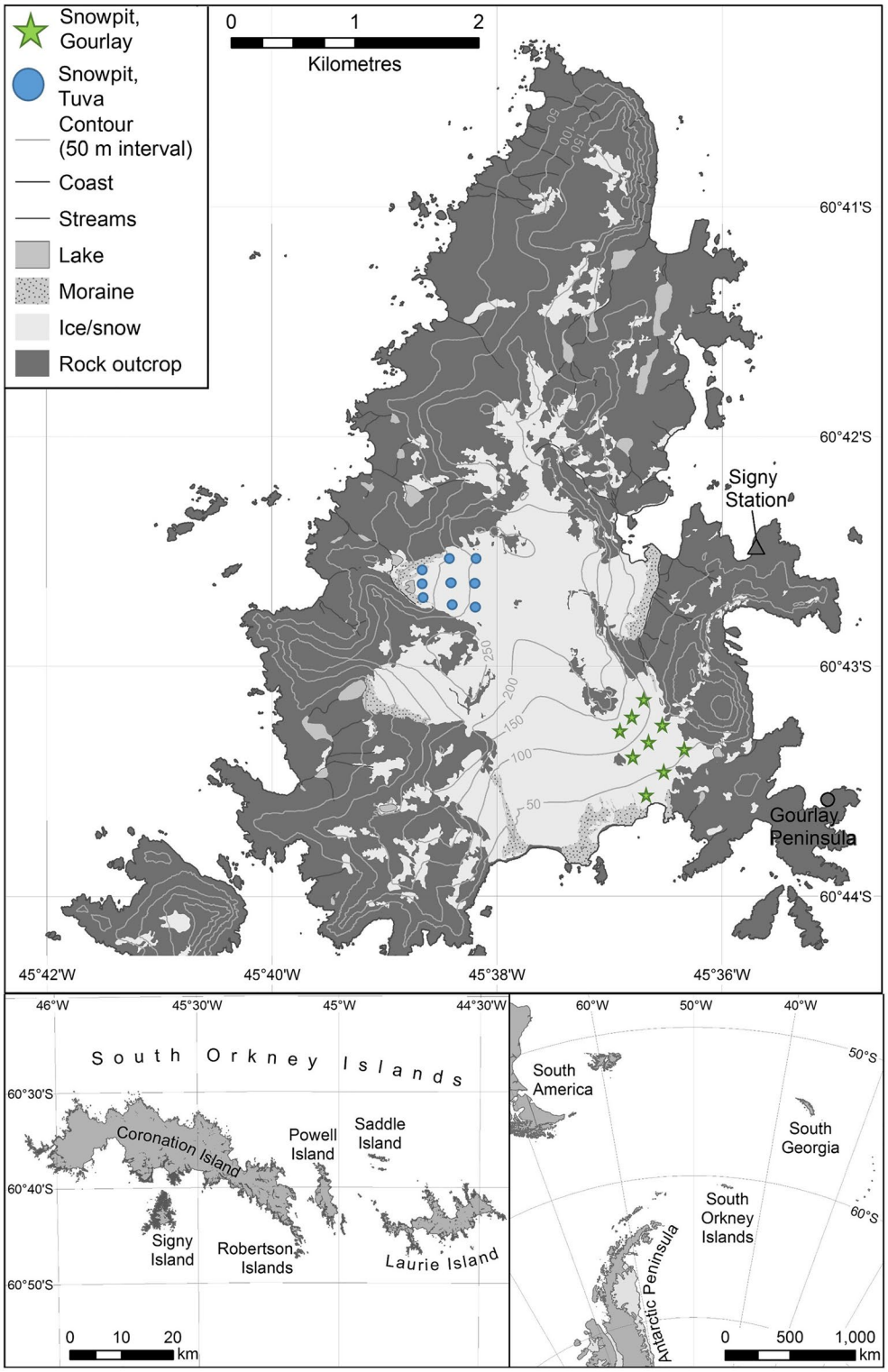

Figure 1. Signy Island and the snow pit sampling sites at Gourlay and Tuva snowfields.

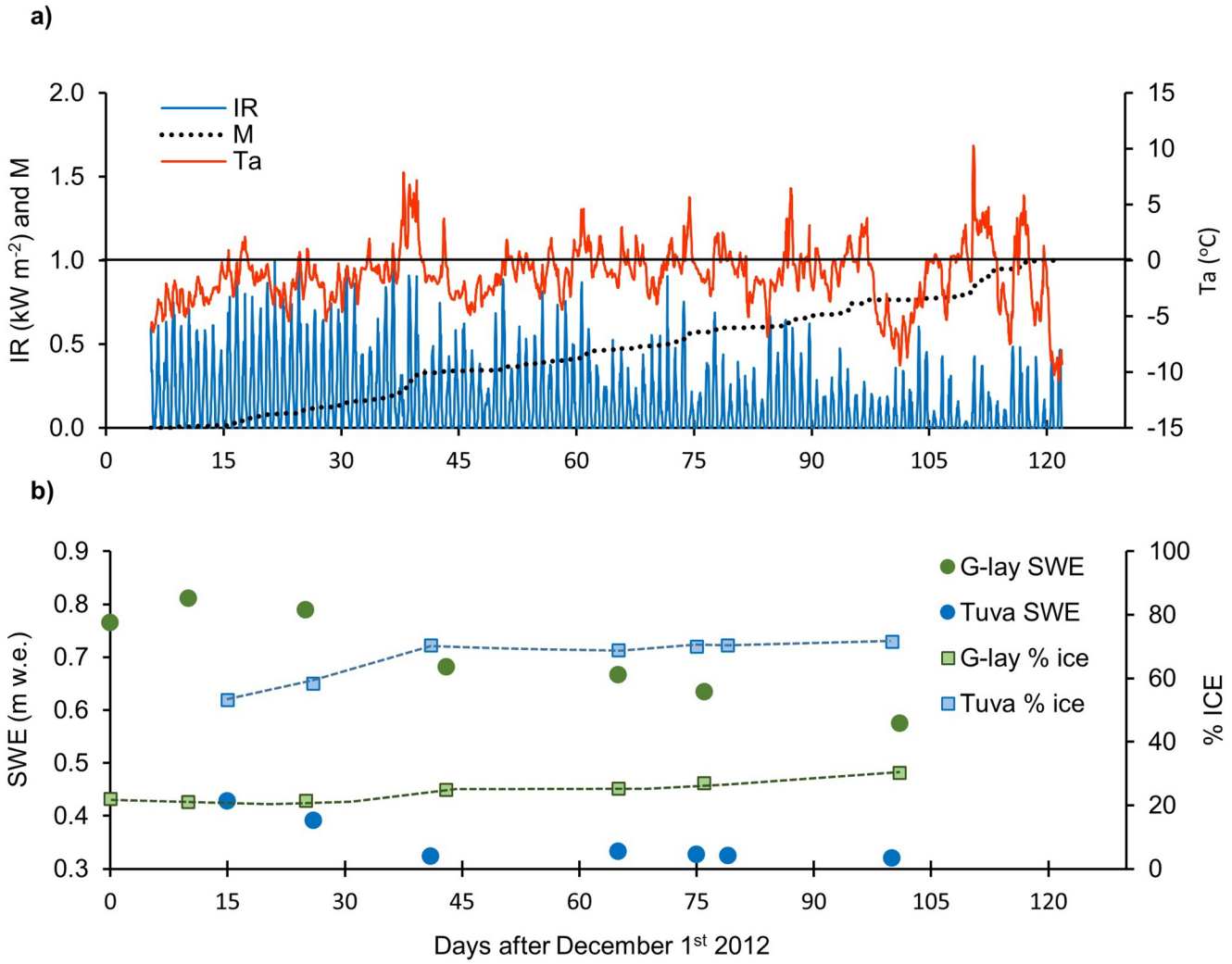

Figure 2. Meteorological variations at 40 m elevation on the Gourlay snowfield (a) and snowpack water equivalent (SWE) changes at both sites throughout the observation period (b). Ta is the air temperature, IR is the incident radiation and M is the cumulative fraction of total observed melt (distributed through time using the Brock and Arnold (2000) surface energy balance model). "ICE" is the percentage of the total SWE present as a basal ice layer.

For both DOC and TDIC, a 50 mL aliquot was filtered through a Whatman GFF filter paper (notional pore space: 0.7 μm) and stored in pre-rinsed 40 mL glass vials for DOC analyses using the membrane conductometric method. This employed a Sievers 5310 Analyzer with UV and persulphate digestion detection limit 0.01 mg L^{-1} and <5% precision errors according to repeat analysis of mid-range (0.4 mg L^{-1}) standards. For NH_4^+ we employed the fluorescence technique described by Taylor et al. (2007), using a Turner Instruments Aquafluor fluorometer, with a 375 nm excitation LED and a 420 nm long pass filter for emission detection. The samples were incubated for typically 3–5 h in order to optimize the intensity of the fluorescence, which enabled a detection limit of 0.7 μg L^{-1} and <5% precision errors according to repeat analysis of 100 μg L^{-1} standards. The same device was also used to provide an optical measure of the concentration of fluorescent DOC at the same excitation/emission wavelengths in the filtered samples. Untreated samples were allowed to equilibrate to room temperature and the average of three fluorescence readings taken at the same wavelengths used for the NH_4^+ detection. These excitation/emission wavelengths are used as an industry standard for the detection of chromophoric dissolved organic matter or "CDOM" and readings are used here to qualitatively assess changes in DOC.

2.4. Ecosystem Production

Attempts were made to measure primary production at all sites during the mid-December, mid-January and mid-February surveys, but several were unsuccessful due to freezing conditions. Very stringent controls upon the use of radionuclides imposed by the British Antarctic Survey meant that freezing conditions conducive to breakage of the vials were to be avoided. Furthermore, measures were to be taken to ensure containment of any leakage in the event of an unexpected breakage (see below). For these reasons, successful results are reported only for mid-December (both sites), mid-February (Tuva only) and mid-March (an additional, opportunistic survey conducted at Gourlay). This means the representativeness of our results is questionable and so we refer to them as measures of "Potential Primary Production." Primary production experiments were conducted in three pits at each site, forming up-slope transects in the direction of the melt gradient. Snow samples of TOP and MID layer were collected from the pits and melted overnight. 150 mL of melted snow was decanted into a borosilicate bottle to which 7.7 μCi (284.9 kBq) of ^{14}C bicarbonate was added. Five replicates were used for each sample: three clear bottles (live), one dark bottle that did not allow any light penetration ("dark") and a clear bottle ("kill") to which filtered buffered paraformaldehyde was added (5% concentration of final volume). Microorganisms in the kill control bottle were killed prior to the addition of the ^{14}C isotope. All bottles were placed upon clear plastic trays filled with snow and returned to the location within the pit from which they were collected for 24 h incubation. Low light conditions were ensured when handling the samples by using a shelter. Isotope was added just prior to the experiment on-site.

At the end of the incubation, samples for primary production measurement were put into a dark box and immediately transferred to the Signy laboratory (up to 1 h travel time). Afterward, samples and kill controls were filtered in a dark lab under low pressure (<7 psi) onto 25 mm GFF filters that were then carefully positioned at the bottom of clean glass scintillation vials. 0.5 mL of 3N HCl was added to each vial and samples were dried in a fume hood at 60°C for up to 8 h. Scintillation vials containing dried filters were transported to Sheffield University at room temperature (2 months' travel time). Then, in the laboratory, 10 mL of scintillation cocktail (10 ml of Permafluor scintillation cocktail: Perkin Elmer, Cambridge, UK) was added to each sample and disintegrations per minute (dpm) were measured on a scintillation counter (Packard Tricarb 3100 TR; Isotech) to calculate the uptake of carbon following Steeman Nielson (1952).

Potential bacterial production (BP) was measured using tritiated leucine uptake following Telling et al. (2010). Briefly: snow and ice were collected into autoclaved and acid-washed 1 L amber HDPE bottles. Samples were melted overnight at 4°C. 1.5 mL of the melted snow or ice was added to 2 mL plastic centrifuge tubes sterilized by autoclaving. Five replicates were used per sample: three live controls and two kill controls. Each sample contained 4.4 μCi (162.8 kBq) of tritiated leucine, with final concentration of 20 nM leucine per sample. Kill controls were killed with addition of 100 μL of 100% cold trichloroacetic acid (TCA) prior to the addition of ^{3}H isotope (to a final concentration 6.25%). Trays with all the control and sample vials were covered in aluminum foil in order to prevent light penetration and placed at the same site of sampling for incubation over 24 h. The incubation was stopped by addition of 100 μL of 100% TCA to the samples. Samples and kill controls were then filtered and kept at 4°C in the dark prior to, and during, 2 months' transportation to the laboratory in Sheffield. 1.5 mL of scintillation cocktail (Monophase®) was then added to each vial before being counted on the scintillation counter. Leucine uptake rate was calculated following Telling et al. (2010).

2.5. Chlorophyll Concentration

Melted snow or ice (up to 900 mL) was filtered under low pressure onto 25 mm GFF filters (combusted at 450°C for 5 h). All sample and filter handling was conducted under low light and low temperature conditions and in an acid-free environment. Filters were stored in glassine envelopes in −80°C until analysis at Signy was conducted 1–8 weeks later, after the intensive field work had been completed. Filters were then added to clean glass scintillation vials with 10 mL of 80% methanol for extraction. Chlorophyll-a standards (*Anacystis nidulans*, Sigma) were made just prior to analysis (0, 1, 2, 5, 10, 50, 100, 200, 500, and 1000 μg L^{-1}). Triplicate measurements were conducted using the Turner Designs Aquafluor fluorometer with excitation at 395 ± 65 nm. The accuracy was tested by repeated use of blanks, chlorophyll standards and a solid standard and the limit of detection was ca. 0.1 μg L^{-1}.

2.6. Cell Enumeration by Flow Cytometry

Ten mL of sample were added to a sterile 15 mL falcon tube and 0.3 mL of buffered formalin (0.2 μm filtered) added immediately after the snow had melted (and no longer than 24 h after collection). Quantitative counting of autotrophic and non-autotrophic cells was then undertaken in the UK using a Partec CyFlow flow cytometer with a single 488 nm laser. Autofluorescence signal events were counted using both fluorescence (Channel FL3) and forward scatter (Channel FSC) measurements. In the first instance, all signal events greater than noise (determined using 0.2 μm filtered samples and deionized water) were counted. Processing then involved gating techniques to isolate events greater than 1 μm to provide the best estimate of intact autotrophic cells. This involved the addition of 1 μm beads to repeat analyses of samples in order to define the gating region for counting. The total number of cells (including bacteria and autotrophs) was then determined following addition and incubation of SYBR Green II stain to the samples. Thereafter, all events on channel FL1 that were greater than "noise" (detected using 0.2 μm filtered and stained blanks) were counted and assumed to include the sum of both autotrophs and heterotrophs within the sample. Potential interference from autofluorescent particles and SYBR Green II binding to detrital material was investigated using bright field and epifluorescence microscopy. This confirmed such interference was present, that it was reduced by the processing described above, but that it also persisted in the final estimates of the autotrophic and non-autofluorescent (i.e., heterotrophic bacteria) cell counts. Therefore, the flow cytometry results are used to provide a broadly representative cell count.

2.7. Partial 16S rRNA Gene Sequencing and Sequence Analysis

Melted snow and ice (500–1500 mL) was filtered onto 0.2 μm Whatman® Nucleopore™ at Signy using a sterilized filtration unit. DNA was isolated from the filter using MoBio PowerWater® DNA isolation kit (MoBio, Inc. Solana, CA, USA) and following the instruction manuals. The highly variable V3/V4 region of the 16S rRNA gene was amplified with bacterial primers S-D-Bact-0341-b-S-17 forward and S-D-Bact-0785-a-A-21 reverse, with overhang Illumina adaptor attached to the primer sequences, creating a single amplicon of ~460 bp The reaction was carried out in 50 μl volumes containing 0.3 mg/mL Bovine Serum Albumin, 250 μM dNTPs, 0.5 μM of each primer, 0.025 U/μL Phusion High-Fidelity DNA Polymerase (Finnzymes OY, Espoo, Finland) and 5X Phusion HF Buffer containing 1.5 mM $MgCl_2$. The following PCR conditions were used: initial denaturation at 95°C for 5 min, followed by 25 cycles consisting of denaturation (95°C for 40 s), annealing (55°C for 2 min) and extension (72°C for 1 min) and a final extension step at 72°C for 7 min. Samples were sequenced using an Illumina MiSeq platform at Liverpool Center for Genomics Research and generated 2 × 300 bp overlapping pair-end reads. The 16S ribosomal RNA gene sequences were clustered into operational taxonomical units (OTUs), based on at least 97% sequence similarity, and assigned taxonomical identification against the SILVA bacterial database. Datasets are deposited on the European Nucleotide Archive under the study accession number PRJNA636650.

3. Results

3.1. Physical Conditions During the Study

Gourlay Snowfield was expected to be a "eutrophic glacier snowpack" due to its close proximity to the Adélie and Chinstrap penguin colonies on Gourlay Peninsula (Figure 1). However, the cold conditions greatly reduced snow melt and the number of penguin chicks that were able to hatch successfully (Dunn et al., 2016). The surface snow albedo also remained high and relatively constant throughout the season (0.73–0.87), such that snow patches lightly discolored (albedo 0.60–0.65) by snow algae only became visible near manured soils in January and February. Both study sites remained snow-covered throughout the whole season and no glacier ice ablation occurred.

Figure 2b shows the evolution of the snow water equivalent (SWE) at each of the sites, and its distribution between snow and superimposed ice. The average initial SWE at Gourlay (0.77 + 0.18 m w.e.) on December 1 increased to 0.81 ± 0.22 m w.e. by the 11th, just prior to the mid-December survey, before gradually depleting to 0.57 ± 0.18 m w.e. in mid-March. Throughout this depletion period, the proportion of SWE present as superimposed ice grew from 21.9 ± 4.4% to 30.2 ± 8.5%. By contrast, Tuva Glacier, located on the western side of the ice cap, accumulated much less snow: 0.43 ± 0.05 m w.e. in mid-December, which was

reduced to 0.32 ± 0.05 m w.e. in mid-March. Superimposed ice was a far more significant component of the total SWE at Tuva Glacier, ranging from 53 ± 5.6% to 72 ± 7.5% throughout the field season. Meteorological conditions suggest that this ice layer formed at the beginning of the previous winter accumulation period, and also just prior to the start of the study. Its development during our study almost certainly means that liquid water penetrated to the snow/ice interface at some point prior to our monitoring period, causing visible grain growth and metamorphosis. Later on, liquid water was also observed to sporadically saturate the ice layer, indicating that much of the snow was lying at or close to the melting point from mid-December onwards. However, surface re-freezing was also common during the cold intervals, making the volume of liquid water percolating down through the snow sometimes negligible.

3.2. Snow Biogeochemistry

The chemical conditions within the two snowfields are shown in Figure 3 (see Table S1 for summary statistics). The data are notable for an unexpected decline in average TOP and MID snow pH at almost all sites (Figure 3a). The Gourlay ICE samples did not conform to this trend, and were already acidic according to the mid-December survey. In some individual samples, pH was as low as 3.3 (not shown), necessitating the use of a range of different pH meters and electrodes to confirm the results were accurate. Otherwise, all TOP and MID snows, as well as Tuva ICE samples, showed average pH values typical of poorly buffered snow (i.e., ca. 5.5), before decreasing throughout the summer to values in the range 4.3–4.6. Figure 3b also shows a pronounced increase in NH_4^+ concentration in snow recorded between the mid-December and mid-January surveys. Concentrations of DIC, DOC, and the CDOM fluorescence (Figures 3c–3e) also generally increased throughout the summer. The DOC and DIC concentrations were broadly equivalent in the two snowfields and nearly always below 1 mg L^{-1}, with the notable exception of significantly greater DOC in the ICE samples compared to the TOP and MID snow samples in all surveys at Gourlay ($p < 0.01$). At Tuva, the higher concentrations in the ICE samples were only encountered in the mid-February survey.

Unsurprisingly, given the high albedo of the surface snow, Figure 3f shows that the concentrations of chlorophyll *a* measured in the top snow layers were below the limit of reliable detection (0.1 μg $L^{-}1$) at the start of the summer (range 0–0.024 μg L^{-1}). Although values increased during subsequent surveys (to average values of 0.047 and 0.060 μg L^{-1} at Tuva and Gourlay, respectively), they remained close to the limit of detection. By far the greatest chlorophyll *a* concentrations were observed in the ICE samples at both sites, with absolute maximum values of 2.78 μg L^{-1} measured in ICE at the lower parts of Tuva Snowfield in February (not shown). Average chlorophyll *a* concentrations in the ICE layer increased from 0.029 to 0.789 μg L^{-1} at Gourlay and from 0.138 to 1.267 μg L^{-1} at Tuva between the mid December and February surveys. The MID snow layer concentrations showed the same seasonal development and were also far greater than those observed in the TOP snow, reaching 0.400 and 0.649 μg L^{-1} by mid-february at Gourlay and Tuva snowfield, respectively.

The input of NH_4^+ responsible for the increase in concentration between mid-December and mid-January (see Figure 3b) was quantified using a mass balance approach. Therefore, at each snowpit, the mass loading of NH_4^+ (in g NH_4-N m^{-2}) was estimated for separate TOP, MID, and ICE samples using the product of their NH_4^+ concentration (in g N m^{-3}) and water equivalent (in m) measurements. The values were then summed at each snowpit and averaged for the mid-December and mid-January surveys. The difference between these means was assumed to represent the net balance of inputs and outputs at each site. An estimate of the runoff export (output) of NH_4^+, also in g NH_4-N m^{-2}, was then derived for this interval from the product of SWE change (Figure 2b) and average NH_4^+ concentration in runoff (0.050 ± 0.0057 mg L^{-1}, $n = 23$: data not shown). We only used runoff samples collected at the margin Tuva Glacier because the runoff at Gourlay was heavily influenced by seals and access became difficult. The results are shown in Table 1, which indicates that the net gain in NH_4^+ at Tuva was approximately twice that at Gourlay. The difference was most likely caused by enhanced deposition at Tuva snowfield, because the runoff export of NH_4^+ was trivial at both sites during this period of the summer season, and no other sources of NH_4^+ were likely.

Table 1 also shows the rate of change in chlorophyll *a* mass loading (i.e., mg Chl *a* m^{-2}), calculated using a similar mass balance approach to that employed for NH_4^+, but for the entire summer (because, unlike NH_4^+ concentrations, the increase in Chlorophyll *a* concentrations was sustained throughout the entire field period). The net change between the mid-December and mid-February chlorophyll *a* values indicated

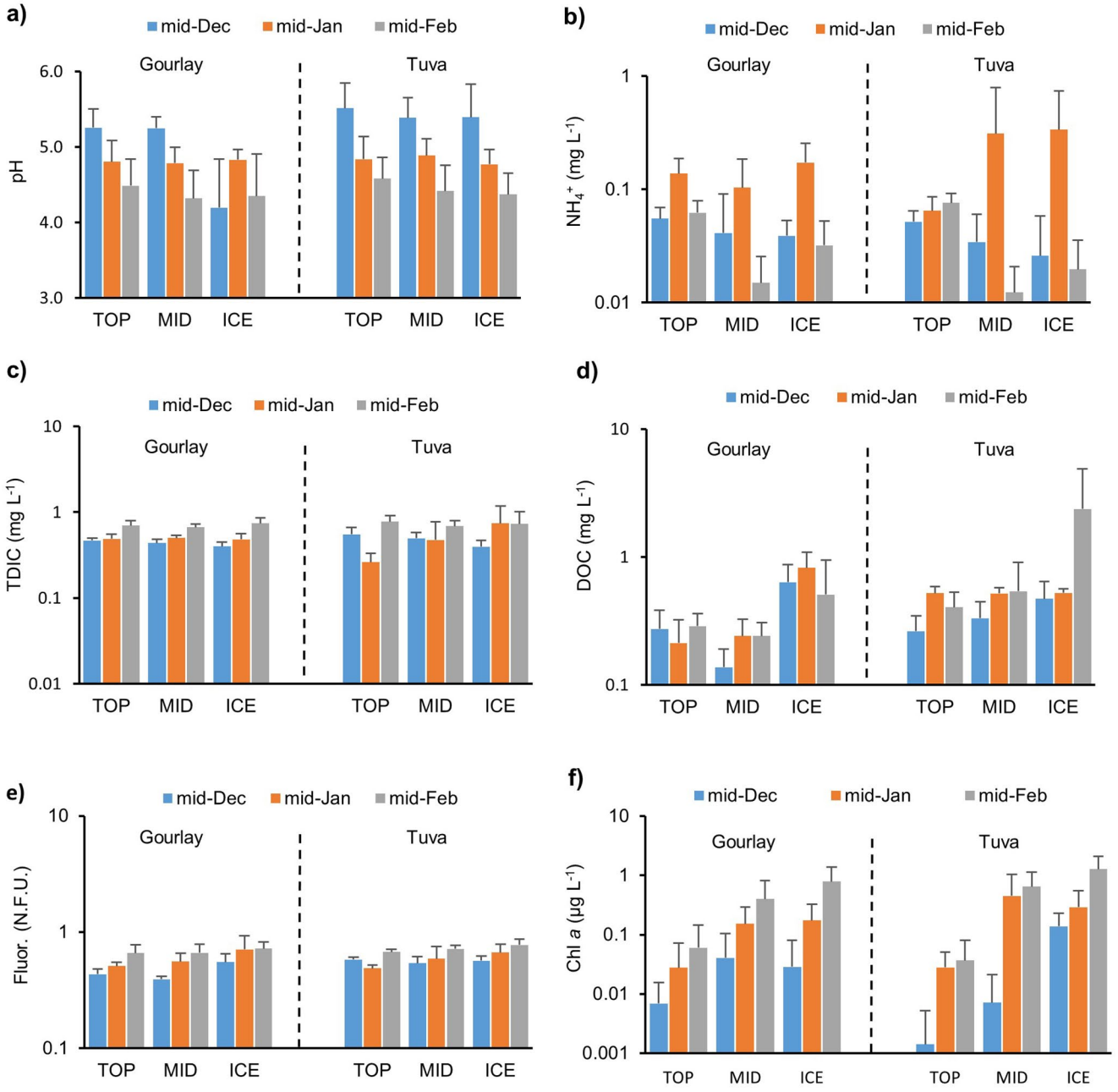

Figure 3. Key biogeochemical parameters for the TOP, MID, and ICE samples during each survey (in mid-December, mid-January, and mid-February). "Fluor." is the fluorescence measurement in notional units ("N.F.U."). Error bars are standard deviations ($n = 9$).

average daily increases of 4.0 and 4.9 µg Chl *a* m^{-2} day^{-1} at Gourlay and Tuva, respectively (Table 1, Figure S1). However, this is an under-estimate of chlorophyll *a* production on account of the likely export of chlorophyll *a* by runoff ("sloughing"), which became important during January (see Figure 2). As for NH_4^+, this output was estimated from the product of the SWE depletion at each site and the flow-weighted mean chlorophyll *a* concentration of outflow from Tuva snowfield (0.446 ± 0.320 µg L^{-1}, $n = 20$, data not shown). The average daily runoff chlorophyll *a* flux proved to be appreciable (1.33 and 0.76 µg Chl *a* m^{-2} d^{-1}) over the interval December 15, 2012 to February 15, or 25 and 13% of total chlorophyll *a* budget at Gourlay and Tuva, respectively. Table 1 shows that accounting for this removal process resulted in very similar rates of average daily chlorophyll *a* production: 5.3 µg Chl *a* m^{-2} d^{-1} at Gourlay, and 5.7 µg Chl *a* m^{-2} d^{-1} at Tuva.

Table 1
Average Daily Ammonium Assimilation and Chlorophyll a Production During the Observation Period

Flux	Gourlay	Tuva
Average daily NH_4 budget, mid-December–mid-January		
Net NH_4-N gain (mg NH_4-N m^{-2} d^{-1})	1.16	2.42
Runoff NH_4-N export (mg NH_4-N m^{-2} d^{-1})	0.213	0.135
NH_4-N deposition (mg NH_4-N m^{-2} d^{-1})	1.37	2.56
Average daily chlorophyll *a* budget, mid-December–mid-February		
Net Chl *a* production (μg Chl a m^{-2} d^{-1})	4.00	4.90
Runoff (μg Chl *a* m^{-2} d^{-1})	1.33	0.76
Gross Chl *a* production (μg Chl a m^{-2} d^{-1})	5.33	5.66
% lost as runoff	25	13
Primary production from Chl *a* (μg C m^{-2} d^{-1})	29.4	30.9

Note. Estimates of runoff fluxes are also used to prevent over-estimation of ammonium assimilation, and under-estimation of chlorophyll a synthesis.

3.3. Potential Primary and Bacterial Production

Due to the weather conditions, potential primary production rates were only assessed using ^{14}C-bicarbonate incorporation during mid-December (both sites), mid-February (Tuva only) and mid-March (Gourlay only). Table 2 shows that the mid-December rates of carbon incorporation by primary producers were close to zero and lay in the range 0.01–0.1 μg C L^{-1} d^{-1} according to average values, although these values suffer from very high standard deviations imposed by spatial variations. The production rates remained low at Tuva even in late season (0.0030–0.25 μg C L^{-1} d^{-1}) but increased significantly at Gourlay (1.16–23.3 μg C L^{-1} d^{-1}), where we measured rates of up to 53.1 μg C L^{-1} d^{-1} in the MID snow layer (not shown). Interestingly, the rates of carbon incorporation via photosynthesis were consistently higher in the MID layer of the snow pits compared with the surface (TOP layer).

Potential BP rates were successfully measured during all of the monthly surveys because non-breakable plastic flasks were used. Across all surveys and sample types, average rates lay in the range 0.2–2,000 μg C L^{-1} d^{-1}, although again, they showed very substantial standard deviations due to spatial variability. However, at Gourlay, values measured in the ICE layer were consistently high relative to both snow layers (although the MID snow layer also demonstrated high values during the February survey). At Tuva, high values were also seen in the ICE layer, but they were almost matched by potential BP rates in the MID snow layer in December and March. Rates of potential BP in the MID snow layer also exceeded the ICE layer in January. Combining all layers, peak BP occurred at Tuva in January and was nearly an order of magnitude lower during the other months. By comparison, peak BP at Gourlay was greatest in February.

3.4. Flow Cytometry and Cell Abundance

Figure 4 shows statistically significant increases in both the concentration (cells mL^{-1}) and loading (cells m^{-2}) of autotrophic and bacterial cells each time a new survey was undertaken at Gourlay. At Tuva snowfield, statistically significant increases were recorded between the first and the second survey (i.e., mid-December to mid-January), but the final survey showed significantly fewer autotrophs and bacterial cells remained by mid-February. Average concentrations across the two snowfields lay in the ranges of 130–520 cells mL^{-1} for autotrophs, and 1,400 to 16,000 cells mL^{-1} for bacteria (Table S3). The proportion of the total cell population represented by autotrophic cells decreased during each successive survey from ca. 8% to 2% at Gourlay, and from 5% to 2% at Tuva. These results indicate bacterial cell proliferation throughout the summer, as is also discernible from Figure 4. The changes in autotroph abundance largely agree with the changes in chlorophyll *a* shown in Figure 3f, with the exception of the marked decline in autotrophic cells at Tuva during the February survey. Reasons for this difference were sought but remain unclear, perhaps reflecting differences in the size distribution of the cells and their relative chlorophyll *a* content. There were

Table 2
Average ± Standard Deviation Rates (n = 3) of Primary Production (PP) and Bacterial Production (BP) According to Rates of Radiolabel Incorporation

		December (μg C $L^{-1}d^{-1}$)		January (μg C $L^{-1}d^{-1}$)		February (μg C $L^{-1}d^{-1}$)		March (μg C $L^{-1}d^{-1}$)	
Site/layer		PP	BP	PP	BP	PP	BP	PP	BP
Gourlay	TOP	0.0089 ± 0.0041	2.04 + 1.60	–	1.10 ± 0.879	–	6.06 ± 6.54	1.16 ± 0.40	1.07 ± 1.29
Gourlay	MID	0.012 ± 0.011	2.79 + 2.82	–	0.22 ± 0.00	–	574 ± 608	23.3 ± 26.0	5.02 ± 2.88
Gourlay	ICE	–	95.5 + 131	–	15.4 ± 5.15	–	608 ± 311	–	45.7 ± 41.7
Tuva	TOP	0.0025 ± 0.0042	4.54 + 7.86	–	20.3 ± 17.6	0.058 ± 0.045	52.7 ± 91.3	–	17.6 ± 28.5
Tuva	MID	0.068 ± 0.098	7.44 + 9.33	–	1969 ± 1900	0.247 ± 0.339	59.0 ± 78.7	–	379 ± 609
Tuva	ICE	–	10.3 + 7.93	–	1409 ± 1320	–	456 ± 303	–	520 ± 498

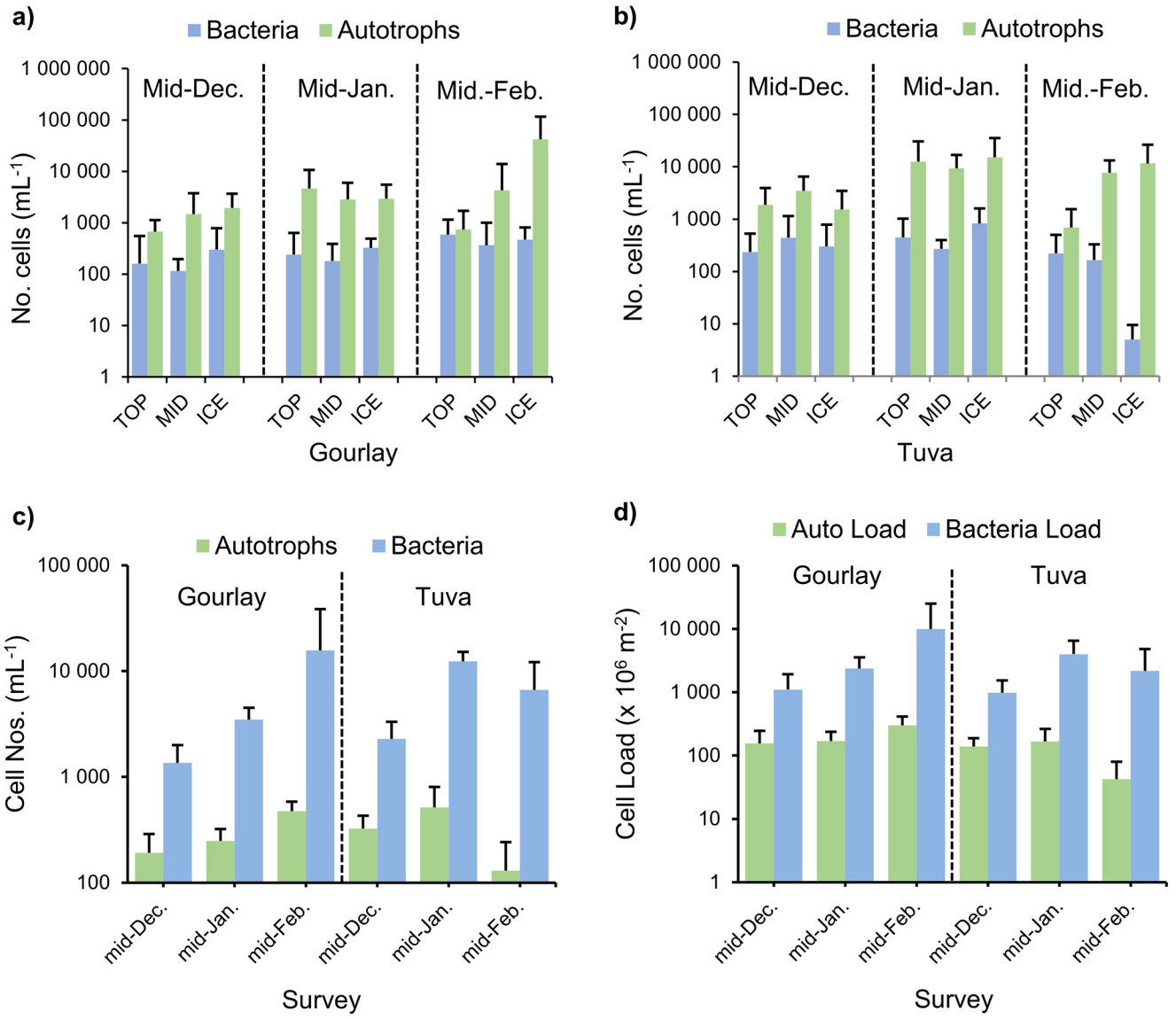

Figure 4. Best estimates of the autotrophic and bacterial cell abundance according to the flow cytometry: (a) and (b) cell concentrations in the TOP, MID, and ICE layers at Gourlay and Tuva, respectively, (c) total cell concentrations at both sites, and (d) total areal cell density or load at both sites.

limited differences between the sites with respect to their concentrations of autotrophic cells in TOP, MID, and ICE samples (data not shown). However, bacterial cells were generally more abundant in ICE samples, especially at Gourlay.

3.5. Bacterial Community Composition From 16S rRNA Gene Analysis

Statistical analysis of the OTU distribution revealed no significant differences in the bacterial community composition across the two glaciers. Nor were differences found between different snow pits at each glacier. By contrast, Analysis of Molecular Variance showed that the community composition of the superimposed ice layer (ICE) was significantly different to both the TOP ($F = 4.7$, $p < 0.001$) and the MID snow layer ($F = 2.97$, $p = 0.04$). There were no significant differences in the community composition between the TOP and MID layers ($F = 0.72$, $p = 0.8$) of snow, however. The community composition was also significantly different in mid-December compared to the other months, even when averaged across all of the habitats. Another significant intra-seasonal change occurred from mid-January to mid-March, providing further

evidence that there were seasonal shifts in the community compositions that were happening in all the snow and ice layers.

The superimposed ice (ICE) was the least diverse habitat according to Inverted Simpson index (average 1/D = 3–8), despite having the highest concentration of cells and nutrients. The ICE layer was initially composed mostly of psychrophilic, heterotrophic bacteria dominated by the genera *Flavobacterium* (Bacteroidetes) and *Cryobacterium* (Actinobacteria). Together, these contributed to 94% of all the 16S rRNA gene sequence reads in December (78% from *Flavobacterium*, 16% from *Cryobacterium*). From January onwards, the diversity increased and the initially dominant *Flavobacterium* decreased markedly (to 0% of reads in March). Other microorganisms, particularly *Chryseobacterium*, *Pedobacter* (both Bacteroidetes) and *Salinibacterium* (Actinobacteria) started to dominate. The microbial composition of the Tuva ICE layer at the onset of the season (December) was also mainly composed of *Flavobacterium* and *Cryobacterium*, and only from January onwards did we observe an increase in diversity, in the form of taxa from the family Sphingobacteriaceae and genus *Chryseobacterium* (data not shown).

The student *t*-test comparison of the different taxonomic groups between Gourlay and Tuva ICE layers revealed that Acidobacteriaceae and Acetobacteriaceae were significantly ($p < 0.05$) more prevalent in Tuva ICE; whilst Microbacteriaceae and the genera *Pedobacter*, *Sphingomonas*, *Salinibacterium*, and *Cryocola* were significantly more prevalent in the Gourlay ICE layer. The Tuva ICE also contained members of the candidate division TM7 (up to 13% of reads), which were not detected at Gourlay. On average, we observed higher concentration of cyanobacteria at Tuva, particularly in January, where the genus *Leptolyngbya* accounted for 50% of all sequence reads. At Gourlay, cyanobacteria in ICE were only present in December (8% of reads).

The TOP and MID snow layers contained more diverse bacterial communities compared to the ICE at both studied sites, consisting of Proteobacteria, Actinobacteria, Firmicutes, and Bacteroidetes. Firmicutes were readily found in the snow layers at both Gourlay and Tuva, but never in the ICE. The Gourlay MID layer seemed transient between the ICE and the TOP layer, for example containing a high proportion (32.7%) of Bacterioidetes sequences most likely inherited from the ICE layer by the end of the season. This difference was not as distinct at Tuva, where the snow layers were much thinner and therefore more likely to be mixed. Furthermore, *Sphingomonas, Cryocola*, and *Pedobacter* were significantly more abundant at Gourlay, while *Acinetobacter* was more common at Tuva.

Links between the bacterial community composition and the biogeochemical conditions described above were sought using distance-based linear modeling ("DistLM") using PRIMER6/PERMANOVA software (PRIMER-E Ltd). In so doing, we tested the relative importance and significance of pH, NH_4^+, chlorophyll *a*, DOC and fluoresence. At Gourlay, stepwise selection of the predictors showed a highly significant influence from pH ($p = 0.0017$), followed by fluorescence ($p = 0.0345$). Neither NH_4^+ nor chlorophyll *a* were significant, whilst DOC was only significant when considered as a lone predictor (i.e., in a marginal test). At Tuva snowfield, pH was also a significant predictor following stepwise selection ($p = 0.0039$), although DIC was more significant ($p = 0.0013$). No other biogeochemical parameters were significant following stepwise selection in the Tuva model (although pH, DIC and chlorophyll *a* were in marginal tests). Overall, the stepwise parameter selection resulted in models that explained 19% and 27% of the variance at Gourlay and Tuva snowfield, respectively.

4. Discussion

The results described above present a clear case for a coupled snowpack-icing ecosystem capable of both autotrophic and heterotrophic production at all depths. The key attributes of our results that describe this ecosystem include: (a) marked changes in the biogeochemical conditions within the snow, revealing nitrogen enrichment from external sources and a strong acidification effect, (b) significant gains in autotrophic cells, resulting in an order of magnitude increase in Chlorophyll *a* loading; and (c) distinct shifts in bacterial community composition and an order of magnitude increase in bacterial cell abundance that out-paced autotrophic cell proliferation. In the discussion below, we argue that these attributes are likely to have been heavily influenced by the cool, wet summer conditions, whose frequent snowfalls and high winds most likely suppressed photosynthesis and forced the bacterial community to respond to acidifying processes that (to

our knowledge) resulted in the lowest pH conditions yet reported in Antarctic snow. Thereafter, we estimate areal rates of primary and bacterial production in the two snowfields, initiating a much-needed assessment of the carbon balance of glacial snowpack ecosystems in the maritime Antarctic.

4.1. Acidification and Nitrogen Dynamics in Snow and Ice Habitats

The onset of breeding at the penguin colony, although greatly suppressed by the weather in the study season, caused a marked increase in NH_4^+ concentrations that was observed between the first two snowpack surveys (Figure 3) and is a typical response to aerosol emissions from guano in coastal Antarctica (Legrand et al., 1998). The subsequent decline in NH_4^+ concentrations between the mid-January and mid-February surveys shows that assimilation and runoff export began to out-pace the fertilization effects of aerosol deposition, as was also demonstrated using detailed nitrogen mass balance measurements on Tuva snowfield in 2003 (Hodson, 2006). These two pathways probably accounted for much of the deposited NH_4^+ because its re-emission as ammonia ($NH_{3[g]}$) will have been suppressed by the low pH conditions. Extrapolating the average daily estimates for NH_4^+ deposition shown in Table 1 to a notional 75 days active (summer) period indicates total summertime deposition rates of 0.103 and 0.192 g NH_4-N m^{-2} yr^{-1} at Gourlay and Tuva snowfields, respectively. These values greatly exceed those for Tuva snowfield during the warmer 2002/2003 (0.028 g NH_4-N m^{-2} yr^{-1}: Hodson, 2006) and also exceed the total dissolved inorganic nitrogen inputs (i.e., NH_4^+ and NO_3^-) for non-glacierised parts of the island (ca. 0.065 gN m^{-2} yr^{-1}) estimated by Christie (1987). Therefore, contrary to expectation, conditions during our study seemed to enhance ammonia emissions from the penguin colony, and might therefore be linked to the unusual acidification process that was also witnessed, but was not detected during the earlier study in 2002/2003.

Studies of runoff from penguin rookeries have shown that nitrification of guano-derived NH_4^+ is an important acidifying mechanism (Tatur & Myrcha et al., 1983). We therefore looked for evidence of nitrification in the snow by examining the concentrations of product NO_3^- using ion chromatography analysis (Table S2). Concentrations were consistently ≤0.12 mg L^{-1} and so the process was ruled out in within the snowpack. This was not surprising, because it is known that nitrification upon Signy Island favors sedimentary habitats such as glacier moraines, periglacial talus and proglacial floodplains (Hodson, 2006). Furthermore, known nitrogen-fixing bacteria (i.e., Nitrosomonadaceae) were conspicuous for their absence in the bacterial communities of the two snowpacks. Similarly, a lack of non-marine SO_4^{2-} was also found during the ion chromatography analysis (Table S2), causing low SO_4^{2-}:Cl^- ratios that suggest dimethyl sulfate degradation (DMS) into methane sulfonic acid and SO_4^{2-} was also an unlikely cause of the acidification. This seems intuitive, given that DMS emissions are dominated by marine biogenic sources (e.g., King et al., 2019), which would have been suppressed by the expansive sea ice conditions all summer.

Given the above, alternative organic acids require consideration, and the greatly increased NH_4^+ deposition means guano-derived oxalic acid and acetic acid are most plausible, although the presence of uric acid from un-processed guano particles is also possible, especially at Gourlay snowfield. Unfortunately, we did not include organic acid analysis in our experimental design. A strong association between NH_4^+, oxalic acid and acetic acid has already been linked to penguin colonies in studies of firn chemistry on the maritime Antarctic Bouvet Island (King et al., 2019) and studies of aerosol chemistry on continental Antarctica (Legrand et al., 1998). Legrand et al. (2012) also emphasize how acid production in aerosol is enhanced by summers with frequent, wet snowfall and melting conditions, because they maintain high levels of moisture in the guano that promote its bacterial decomposition. Such conditions were clearly prevalent during our study and so guano emissions represent the most plausible cause of the unexpected snowpack acidification, especially with respect to the TOP and MID snows. The ICE layer at Gourlay probably developed acidity earlier than the overlying snow (and the ice layer at Tuva snowfield) because its proximity to the penguin colony would have enabled contact with guano-derived aerosol and particles blown directly on the glacier surface during the previous summer. However, further (carbonic) acidity linked to bacterial respiration of CO_2 should also be considered, because the TDIC concentrations in Figure 3c show seasonal increases, especially at Gourlay, along with high concentrations in the ICE layer.

4.2. Relationship Between Bacterial Community, Guano, and Snowpack Acidity

A comparison of the bulk 16S rRNA gene data set presented in this study with similar data from snows of the Antarctic Peninsula and Livingston Island (South Shetland Islands, Antarctica) has already been undertaken by Malard et al. (2019). This work showed prominent differences between the bacterial community composition within all three regions, and a greater number of OTUs upon the two islands. Since the sites upon the Antarctic Peninsula were all at high elevation, it seems likely that the island snowpack ecosystems are more influenced by their surrounding soil and marine ecosystems. The analysis presented by Malard et al. (2019) suggested that soil is most influential, which is also consistent with the likely effects of persistent sea ice cover around Signy Island during our study. Stronger than usual effects of the resident penguin colony and its ornithogenic soils therefore seem likely. Although, we reported the presence of many cosmopolitan bacteria, the dominant taxa described in a study of Adélie penguin guano (namely the Moraxellaceae/Pseudomonadaceae, Flavobacteriaceae, and the Micrococcaceae: Zdanowski et al., 2004) represented six (Gourlay) and seven (Tuva) of the 15 most abundant groups found in the Signy Island snow. Of the other abundant groups in our samples, the Oxalobacteraceae are particularly important, especially *Ralstonia*, which is known to include species that are metabolically diverse in East Antarctic snow (Antony et al., 2012) but highly likely to be capable of oxidizing oxalic acid from guano. The presence of these groups and also the significance of pH in the distance-based linear modeling of bacterial community composition at both snowfields clearly support the assertion that guano-derived aerosol deposition was a key driver of bacterial cell proliferation in the snow. Furthermore, the distance-based linear modeling showed little evidence for a dependence of the bacterial community upon autotrophic production (as represented by chlorophyll *a*). However, our results still require cautious interpretation because studies demonstrating the sensitivity of soil bacterial communities to pH are common and might reflect that a number of different processes are responsible, even upon Signy Island (Chong et al., 2010). More direct studies of guano-fertilization and acidification in maritime Antarctic snow ecosystems are clearly warranted.

4.3. Seasonal Bacterial Production

Estimates of potential BP in Table 2 are extremely variable, lying in the range 0.2–2000 μg C L^{-1} d^{-1}. The variability is to some extent caused by the very heterogeneous distribution of bacteria in the snow and ice, as depicted by the large standard deviations in Figures 4a and 4b (see also Table S3). As a consequence, with one outlier removed, the rates of BP in Table 2 were significantly correlated ($r = 0.82$, $p < 0.05$, $n = 16$) with the average cell concentration in the samples that were incubated. The relationship took the form:

$$\mathrm{BP} = 9.0 \times 10^{-5} \mathrm{BCC}^{1.63} \quad (1)$$

where BP represents the bacterial production data in Table 2 and BCC is the average bacterial cell concentration of the three samples used in the incubations and estimated using flow cytometry. Since incubations could not be undertaken at all snowpit sites, the relationship in Equation 1 was used to predict BP whilst accounting for spatial variability at the two snowfields. The product of the predicted BP and the snow water equivalent was then used to estimate bacterial carbon fixation on an areal basis (i.e., mg C m^{-2} d^{-1}), which is presented in Table 3. This shows that the greatest BP rates occurred after December, especially in the ICE layer. By contrast, low rates of BP in the TOP layer occurred, whilst the MID layer was least variable and broadly similar at the two sites. Comparison with the rates of primary production, also in Table 3 and discussed below, demonstrates a net-heterotrophic ecosystem, thus supporting the notion that respired CO_2 contributed to local acidification and helping to explain the general increase in TDIC shown by Figure 3c.

4.4. Chlorophyll and Primary Production

Data for common, morphologically similar red snow algal species to those that were dominant in the present study allow crude estimation of the seasonal primary production using the chlorophyll *a* accumulation rates in Table 1. Thus, a chlorophyll *a* content of ca. 0.28 ± 0.11 mg g^{-1} dry mass (Davey et al., 2019), a dry mass density of 1,400 kg m^{-3} (Dauchet et al., 2015) and a carbon content of 0.02 μg C mm^{-3} (Fogg, 1967), produced carbon fluxes of 29.4 and 30.9 μg C m^{-2} d^{-1} for Gourlay and Tuva snowfields respectively.

Table 3
Areal Estimates of Bacterial Production and Primary Production

	Mid-December		Mid-January		Mid-February	
Site/layer	BP	PP	BP	PP	BP	PP
Gourlay (mg C m^{-2} d^{-1})						
TOP	0.38 ± 0.26	$1.1 \times 10^{-4} \pm 3.2 \times$ 10-4	9.1 ± 12	0.0032 ± 0.048	0.45 ± 0.59	0.0073 ± 0.013
MID	7.1 ± 12	0.037 ± 0.045	16 ± 19	0.24 ± 0.25	27 ± 63	1.3 ± 2.2
ICE	3.4 ± 3.2	0.053 ± 0.051	6.8 ± 6.2	0.086 ± 0.074	530 ± 941	0.65 ± 0.56
All	11 ± 12	0.091 ± 0.23	32 ± 22	0.33 ± 0.37	550 ± 70	2.0 ± 2.32
Tuva (mg C m^{-2} d^{-1})						
TOP	1.9 ± 2.1	$3.9 \times 10^{-5} \pm 1.1 \times 10^{-4}$	44 ± 64	0.0030 ± 0.0024	0.40 ± 0.52	0.0044 ± 0.0043
MID	12 ± 11	0.0015 ± 0.0029	27 ± 22	0.15 ± 0.17	20 ± 16.2	0.20 ± 0.17
ICE	3.3 ± 4.2	0.11 ± 0.0075	140 ± 190	0.31 ± 0.26	89 ± 120	2.6 ± 1.5
All	17 ± 11	0.11 ± 0.27	210 ± 70	0.46 ± 0.54	110 ± 19	2.8 ± 1.2

Note. Estimated from the distribution of radiolabel incorporation rates across the two snowfields using Equations 1 and 2.

Significant errors would be attributable to these calculations if a cyanobacterial population played a large role in primary production, and it is appreciated that significant differences in the chlorophyll *a* content of snow algae can occur (see Davey et al., 2019). However, microscopy confirmed the predominance of cells analogous in form to *C. reinhardtii* and *C. nivalis* and our molecular data suggest that cyanobacteria were significant contributors only to the ICE layer at Tuva.

Areal rates of daily primary production could also be estimated from the limited number of ^{14}C-bicarbonate incorporation rate measurements (see Table 2) due to their significant correlation ($p = 0.04$, $n = 8$, $r = 0.91$) with the chlorophyll concentration of the snow at the time of the incubations. These estimates are therefore appropriate for comparison with the BP rates in Table 3. The relationship used in this case was:

$$PP = 15.8Chl_a^{1.44} \quad (2)$$

where PP represents the average rates of ^{14}C incorporation for either TOP or MID snow incubations (μg C L^{-1} d^{-1}), and Chl *a* the corresponding chlorophyll *a* concentration following extraction (μg L^{-1}). We therefore applied Equation 2 to the chlorophyll *a* concentrations of the TOP, MID, and ICE layers at Gourlay and Tuva for the December, January and February surveys. As with the preceding BP assessment, the predictions were multiplied by the corresponding water equivalent volume, summed to produce a total for that particular snowpit, and then averaged at each snow field. The results in Table 3 indicate that primary production ranged from minima of 0.091 and 0.11 mg C m^{-2} d^{-1} in mid-December at Tuva and Gourlay respectively, to 2.0 and 2.8 mg C m^{-2} d^{-1} in mid-February. These values are between 3 and 90 times the average daily rates of photosynthesis inferred directly from chlorophyll *a* in Table 1. The large difference most likely results from the creation of rather ideal conditions (i.e., a liquid suspension of cells) every time a radiolabel incorporation experiment was conducted. However, the higher, end of season rates in Table 3 are very close to Fogg's (1967) results on Signy Island (i.e., ca. 10 mg C m^{-2} d^{-1}). His work did not involve melting the snow to create a suspension, but the snow was very likely to have been at the melting point. Further estimates of rates of photosynthesis are also provided for two other snowfields in the Antarctic Peninsula region by Gray et al. (2020). These results, based upon short-term chamber measurements of net ecosystem production over very high green algal densities, seem to imply gross ecosystem photosynthesis rates of between 0.9 and 8.1 mg C m^{-2} h^{-1}, implying an order of magnitude greater daily rate than that estimated by Fogg (1967). However, these estimates were not representative of red snow algae and were derived for surface snows with ca. 10^4 cells mL^{-1} (Gray et al., 2020). These published results do, however, tend to suggest far lower rates of primary production occurred during the present study than is typical during warmer summers or in warmer parts of the Antarctic Peninsula region. The most realistic estimates of average daily photosynthesis

during our study are likely to be the lower estimates derived from Chlorophyll *a* accumulation in Table 3 (i.e., ca. 30 μg C m^{-2} d^{-1}).

Although the experimental conditions of our radioisotope experiments were more favorable for biological production than the real conditions in the snowpack, we see no reason to question the clear outcome that BP exceeded primary production until late summer (see Table 2). This outcome is also supported by the flow cytometry results, which showed that bacterial cells increasingly accounted for the total biomass within the snow and ice layers, representing as much as 98% of the total cell population by the end of the summer. An alternative explanation of the flow cytometry results is that the proliferation was caused by dust deposition of cellular debris and organic matter capable of binding to SYBR Green II. However, no evidence of atmospheric deposition was evident from the TOP snow samples, which would have been enriched the most. It seems far more likely that cold, snowy, conditions favor net heterotrophy on account of the greater resource needs of the larger autotrophic cells, as well as their frequent burial by fresh snow, which reduces light penetration (cf. Jones, 1999). Therefore, the conditions encountered during the our study help demonstrate how the carbon balance of Antarctica's largest terrestrial habitat is very climate-sensitive and requires an appreciation of the microbial processes occurring in snow and ice well below its surface.

5. Conclusions

Our study has presented evidence of a diverse and dynamic microbial community within the snow and refrozen ice layers of maritime Antarctic glaciers, even during a cold summer season with low rates of ablation and frequent snow fall. Microbial diversity and activity were distinct between the different vertical "zones" within the snowpack, which included a surface 20 cm layer subject to repeated erosion/deposition by strong winds and fresh snowfall, a more stable mid-snowpack layer beneath it and an underlying basal ice layer of refrozen snowmelt superimposed upon the glacier surface. The ice layer was the least diverse ecosystem and comprised of many bacteria that are commonly reported as cold region psychrophiles. The snow supported the most diverse bacterial community, dominated by Proteobacteria, Actinobacteria, Firmicutes, and Bacterioidetes. The ice layer was also the most productive, making a contribution to both primary production and BP that was unexpected and highly significant. Together, the ice and the overlying snowpack demonstrated significant, order of magnitude increases in chlorophyll *a* throughout the season, corresponding to an average rate of photosynthesis of ca. 30 μg C m^{-2} d^{-1} when attributed to red snow algae. This demonstrates how detectable rates of primary production can result even when meteorological conditions cause intermittent melting and induce water scarcity. However, under these conditions, the ecosystem is net-heterotrophic. Rates of bacterial production (11–550 mg C m^{-2} d^{-1}) usually outweighed primary production (0.1–2.8 mg C m^{-2} d^{-1}) according to rates of radioisotope incorporation in melted snow samples. This was accompanied by the proliferation of bacterial cells and a reduction in the proportion of autotrophic cells within the community from an initial 5%–8% in mid-December, to 2% by mid-February. An unexpected decrease in pH accompanied this change, and was most likely controlled by the biological production of organic acids associated with guano deposition from a local penguin colony. Changes in bacterial community composition were strongly linked to this acidifying process, and so the bacterial community seemed better adapted to colder summer conditions than the autotrophic community.

Conflict of Interest

The authors declare no conflicts of interest relevant to this study.

Data Availability Statement

The data used in this manuscript are available from the European Nucleotide Archive (https://www.ebi.ac.uk/ena/browser/view/PRJNA636650) and from https://data.bas.ac.uk/metadata.php?id=GB/NERC/BAS/PDC/00933, https://data.bas.ac.uk/metadata.php?id=GB/NERC/BAS/PDC/00989 and https://data.bas.ac.uk/metadata.php?id=GB/NERC/BAS/PDC/00928.

Acknowledgments
The authors acknowledge Natural Environment Research Council (UK) awards NE/H014446/1 and NE/S001034/1, and Research Council of Norway award 288402 (BIOICE). P. Convey is supported by NERC core funding to the BAS "Biodiversity, Evolution and Adaptation" Team. The authors thank Laura Gerrish (BAS Mapping and Geographic Information Center) for preparing the map in Figure 1.

References

Amato, P., Hennebelle, R., Magand, O., Sancelme, M., Delort, A. M., Barbante, C., et al. (2007). Bacterial characterization of the snow cover at Spitzberg, Svalbard. *FEMS Microbiology Ecology*, *59*(2), 255–264. https://doi.org/10.1111/j.1574-6941.2006.00198.x

Antony, R., Mahalinganathan, K., Krishnan, K. P., & Thamban, M. (2012). Microbial preference for different size classes of organic carbon: A study from Antarctic snow. *Environmental Monitoring and Assessment*, *184*(10), 5929–5943. https://doi.org/10.1007/s10661-011-2391-1

Bagshaw, E. A., Tranter, M., Wadham, J. L., Fountain, A. G., Dubnick, A., & Fitzsimons, S. (2016). Processes controlling carbon cycling in Antarctic glacier surface ecosystems. *Geochemical Perspectives Letters*, *2*, 44–54. https://doi.org/10.7185/geochemlet.1605

Bokhorst, S., Convey, P., & Aerts, R. (2019). Nitrogen inputs by marine vertebrates drive abundance and richness in Antarctic terrestrial ecosystems. *Current Biology*, *29*(10), 1721–1727. https://doi.org/10.1016/j.cub.2019.04.038

Brock, B. W., & Arnold, N. S. (2000). A spreadsheet-based (Microsoft Excel) point surface energy balance model for glacier and snow melt studies. *Earth Surface Processes and Landforms*, *25*(6), 649–658. https://doi.org/10.1002/1096-9837(200006)25:6<649::AID-ESP97>3.0.CO;2-U

Cannone, N., Guglielmin, M., Convey, P., Worland, M. R., & Longo, S. F. (2016). Vascular plant changes in extreme environments: Effects of multiple drivers. *Climatic Change*, *134*(4), 651–665. https://doi.org/10.1007/s10584-015-1551-7

Carpenter, E. J., Lin, S., & Capone, D. G. (2000). Bacterial activity in South Pole snow. *Applied and Environmental Microbiology*, *66*(10), 4514–4517. https://doi.org/10.1128/aem.66.10.4514-4517.2000

Chong, C. W., Pearce, D. A., Convey, P., Tan, G. A., Wong, R. C., & Tan, I. K. (2010). High levels of spatial heterogeneity in the biodiversity of soil prokaryotes on Signy Island, Antarctica. *Soil Biology and Biochemistry*, *42*(4), 601–610. https://doi.org/10.1016/j.soilbio.2009.12.009

Christie, P. (1987). Nitrogen in two contrasting Antarctic bryophyte communities. *Journal of Ecology*, *75*, 73–93. https://doi.org/10.2307/2260537

Cook, J. M., Hodson, A. J., Gardner, A. S., Flanner, M., Tedstone, A., Williamson, C., et al. (2017). Quantifying bioalbedo: A new physically based model and discussions of empirical methods for characterizing biological influence on ice and snow albedo. *The Cryosphere*, *11*(6), 2611–2632. https://doi.org/10.5194/tc-11-2611-2017

D'Andrilli, J., Smith, H. J., Dieser, M., & Foreman, C. M. (2017). Climate driven carbon and microbial signatures through the last ice age. *Geochemical Perspectives Letters*, *4*, 29–34. https://doi.org/10.7185/geochemlet.1732

Dauchet, J., Blanco, S., Cornet, J.-F., & Fournier, R. (2015). Calculation of radiative properties of photosynthetic microorganisms. *Journal of Quantitative Spectroscopy and Radiative Transfer*, *161*, 60–84. https://doi.org/10.1016/j.jqsrt.2015.03.025

Davey, M. P., Norman, L., Sterk, P., Huete-Ortega, M., Bunbury, F., Loh, B. K. W., et al. (2019). Snow algae communities in Antarctica: Metabolic and taxonomic composition. *New Phytologist*, *222*(3), 1242–1255. https://doi.org/10.1111/nph.15701

Dial, R. J., Ganey, G. Q., & Skiles, S. M. (2018). What color should glacier algae be? An ecological role for red carbon in the cryosphere. *FEMS Microbiology Ecology*, *94*(3). https://doi.org/10.1093/femsec/fiy007

Dunn, M. J., Jackson, J. A., Adlard, S., Lynnes, A. S., Briggs, D. R., Fox, D., & Waluda, C. M. (2016). Population size and decadal trends of three penguin species nesting at Signy Island, South Orkney Islands. *PLOS One*, *11*(10), e0164025. https://doi.org/10.1371/journal.pone.0164025

Fogg, G. E. (1967). Observations on the snow algae of the South Orkney Islands. *Philosophical Transactions of the Royal Society of London. Series B, Biological Sciences*, *252*(777), 279–287. https://doi.org/10.1098/rstb.1967.0018

Ganey, G. Q., Loso, M. G., Burgess, A. B., & Dial, R. J. (2017). The role of microbes in snowmelt and radiative forcing on an Alaskan icefield. *Nature Geoscience*, *10*(10), 754–759. https://doi.org/10.1038/ngeo3027

Gray, A., Krolikowski, M., Fretwell, P., Convey, P., Peck, L. S., Mendelova, M., et al. (2020). Remote sensing reveals Antarctic green snow algae as important terrestrial carbon sink. *Nature Communications*, *11*(1), 1–9. https://doi.org/10.1038/s41467-020-16018-w

Greenfield, L. G. (1992). Precipitation nitrogen at maritime Signy Island and continental Cape Bird, Antarctica. *Polar Biology*, *11*(8), 649–653. https://doi.org/10.1007/bf00237961

Hodson, A. (2006). Biogeochemistry of snowmelt in an Antarctic glacial ecosystem. *Water Resources Research*, *42*(11). https://doi.org/10.1029/2005WR004311

Hodson, A., Brock, B., Pearce, D., Laybourn-Parry, J., & Tranter, M. (2015). Cryospheric ecosystems: A synthesis of snowpack and glacial research. *Environmental Research Letters*, *10*(11), 110201. https://doi.org/10.1088/1748-9326/10/11/110201

Hodson, A., Paterson, H., Westwood, K., Cameron, K., & Laybourn-Parry, J. (2013). A blue-ice ecosystem on the margins of the East Antarctic ice sheet. *Journal of Glaciology*, *59*(214), 255–268. https://doi.org/10.3189/2013JoG12J052

Hodson, A. J., Nowak, A., Cook, J., Sabacka, M., Wharfe, E. S., Pearce, D. A., et al. (2017). Microbes influence the biogeochemical and optical properties of maritime Antarctic snow. *Journal of Geophysical Research: Biogeosciences*, *122*(6), 1456–1470. https://doi.org/10.1002/2016JG003694

Hoham, R. W., & Remias, D. (2020). Snow and glacial algae: A Review. *Journal of Phycology*, *56*(2), 264–282. https://doi.org/10.1111/jpy.12952

Jones, H. G. (1999). The ecology of snow-covered systems: A brief overview of nutrient cycling and life in the cold. *Hydrological Processes*, *13*(14–15), 2135–2147. https://doi.org/10.1002/(sici)1099-1085(199910)13:14/15<2135::aid-hyp862>3.0.co;2-y

King, A. C. F., Thomas, E. R., Pedro, J. B., Markle, B., Potocki, M., Jackson, S. L., et al. (2019). Organic compounds in a sub-Antarctic ice core: A potential suite of sea ice markers. *Geophysical Research Letters*, *46*, 9930–9939. https://doi.org/10.1029/2019GL084249

Larose, C., Dommergue, A., & Vogel, T. M. (2013). Microbial nitrogen cycling in Arctic snowpacks. *Environmental Research Letters*, *8*(3), 035004. https://doi.org/10.1088/1748-9326/8/3/035004

Lee, J. R., Raymond, B., Bracegirdle, T. J., Chades, I., Fuller, R. A., Shaw, J. D., & Terauds, A. (2017). Climate change drives expansion of Antarctic ice-free habitat. *Nature*, *547*(7661), 49–54. https://doi.org/10.1038/nature22996

Legrand, M., Ducroz, F., Wagenbach, D., Mulvaney, R., & Hall, J. (1998). Ammonium in coastal Antarctic aerosol and snow: Role of polar ocean and penguin emissions. *Journal of Geophysical Research*, *103*(D9), 11043–11056. https://doi.org/10.1029/97JD01976

Legrand, M., Gros, V., Preunkert, S., Sarda Estève, R., Thierry, A. M., Pépy, G., & Jourdain, B. (2012). A reassessment of the budget of formic and acetic acids in the boundary layer at Dumont d'Urville (coastal Antarctica): The role of penguin emissions on the budget of several oxygenated volatile organic compounds. *Journal of Geophysical Research: Atmosphere*, *117*(D6). https://doi.org/10.1029/2011JD017102

Lutz, S., Anesio, A. M., Field, K., & Benning, L. G. (2015). Integrated "omics," targeted metabolite and single-cell analyses of Arctic snow algae functionality and adaptability. *Frontiers in Microbiology*, *6*, 1323. https://doi.org/10.3389/fmicb.2015.01323

Lutz, S., Anesio, A. M., Raiswell, R., Edwards, A., Newton, R. J., Gill, F., & Benning, L. G. (2016). The biogeography of red snow microbiomes and their role in melting Arctic glaciers. *Nature Communications*, *7*, 11968. https://doi.org/10.1038/ncomms11968

Malard, L. A., Šabacká, M., Magiopoulos, I., Hodson, A., Tranter, M., Siegert, M. J., et al. (2019). Spatial variability of Antarctic surface snow bacterial communities. *Frontiers in Microbiology*, *10*, 461. https://doi.org/10.3389/fmicb.2019.00461

Martinez-Alonso, E., Pena-Perez, S., Serrano, S., Garcia-Lopez, E., Alcazar, A., & Cid, C. (2019). Taxonomic and functional characterization of a microbial community from a volcanic englacial ecosystem in Deception Island, Antarctica. *Scientific Reports*, *9*(1), 1–14. https://doi.org/10.1038/s41598-019-47994-9

Matthews, D. H., & Maling, D. H. (1967). *The geology of the South Orkney Islands: I. Signy Island* (Vol. 25). HMSO.

Michaud, L., Giudice, A. L., Mysara, M., Monsieurs, P., Raffa, C., Leys, N., et al. (2014). Snow surface microbiome on the High Antarctic Plateau (DOME C). *PloS One*, *9*(8), e104505. https://doi.org/10.1371/journal.pone.0104505

Noon, P. E., Leng, M. J., & Jones, V. J. (2003). Oxygen-isotope ($\delta^{18}O$) evidence of Holocene hydrological changes at Signy Island, maritime Antarctica. *The Holocene*, *13*(2), 251–263. https://doi.org/10.1191/0959683603hl611rp

Nowak, A., Hodson, A., & Turchyn, A. V. (2018). Spatial and temporal dynamics of dissolved organic carbon, chlorophyll, nutrients and trace metals in maritime Antarctic snow and snowmelt. *Frontiers of Earth Science*, *6*, 201. https://doi.org/10.3389/feart.2018.00201

Remias, D., Pichrtová, M., Pangratz, M., Lütz, C., & Holzinger, A. (2016). Ecophysiology, secondary pigments and ultrastructure of Chlainomonas sp.(Chlorophyta) from the European Alps compared with Chlamydomonas nivalis forming red snow. *FEMS Microbiology Ecology*, *92*(4), fiw030. https://doi.org/10.1093/femsec/fiw030

Smith, H. J., Foster, R. A., McKnight, D. M., Lisle, J. T., Littmann, S., Kuypers, M. M., & Foreman, C. M. (2017). Microbial formation of labile organic carbon in Antarctic glacial environments. *Nature Geoscience*, *10*(5), 356–359. https://doi.org/10.1038/ngeo2925

Steeman Nielsen, E. (1952). The use of radio-active carbon (C^{14}) for measuring organic production in the sea. *Journal de Conseil*, *18*, 117–140. https://doi.org/10.1093/icesjms/18.2.117

Takeuchi, N. (2013). Seasonal and altitudinal variations in snow algal communities on an Alaskan glacier (Gulkana glacier in the Alaska range). *Environmental Research Letters*, *8*(3), 035002. https://doi.org/10.1088/1748-9326/8/3/035002

Tatur, A., & Myrcha, A. (1983). Changes in chemical composition of waters running off from the penguin rookeries in the Admiralty Bay region (King George Island, South Shetland Islands, Antarctica). *Polish Polar Research*, *4*(1), 113–126.

Taylor, B. W., Keep, C. F., Hall Jr, R. O., Koch, B. J., Tronstad, L. M., Flecker, A. S., & Ulseth, A. J. (2007). Improving the fluorometric ammonium method: Matrix effects, background fluorescence, and standard additions. *Journal of the North American Benthological Society*, *26*(2), 167–177. https://doi.org/10.1899/0887-3593(2007)26[167:ITFAMM]2.0.CO;2

Telling, J., Anesio, A. M., Hawkings, J., Tranter, M., Wadham, J. L., Hodson, A. J., et al. (2010). Measuring rates of gross photosynthesis and net community production in cryoconite holes: A comparison of field methods. *Annals of Glaciology*, *51*(56), 153–162. https://doi.org/10.3189/172756411795932056

Thomas, W. H. (1972). Observations on snow algae in California. *Journal of Phycology*, *8*(1). https://doi.org/10.1111/j.1529-8817.1972.tb03994.x

Trusel, L. D., Frey, K. E., Das, S. B., Karnauskas, K. B., Kuipers, P., Munneke, E. M., & van den Broeke, M. R. (2015). Divergent trajectories of Antarctic surface melt under two twenty-first-century climate scenarios. *Nature Geoscience*, *8*, 927–932. https://doi.org/10.1038/ngeo2563

Vaughan, D. G. (2006). Recent trends in melting conditions on the Antarctic Peninsula and their implications for ice-sheet mass balance and sea level. *Arctic Antarctic and Alpine Research*, *38*(1), 147–152. https://doi.org/10.1657/1523-0430(2006)038[0147:rtimco]2.0.co;2

Waluda, C. M., Gregory, S., & Dunn, M. J. (2010). Long-term variability in the abundance of Antarctic fur seals Arctocephalus gazella at Signy Island, South Orkneys. *Polar Biology*, *33*(3), 305–312. https://doi.org/10.1007/s00300-009-0706-2

Zdanowski, M. K., Weglenski, P., Golik, P., Sasin, J. M., Borsuk, P., Zmuda, M. J., & Stankovic, A. (2004). Bacterial diversity in Adelie penguin, Pygoscelis adeliae, guano: Molecular and morpho-physiological approaches. *FEMS Microbiology Ecology*, *50*(3), 163–173. https://doi.org/10.1016/j.femsec.2004.06.012